



Design, synthesis, and antitumor activity evaluation of carbazole derivatives with potent HDAC inhibitory activity

Likun Sun¹ · Leiqiang Han² · Liang Zhang³ · Chen Chen¹ · Chengyun Zheng¹

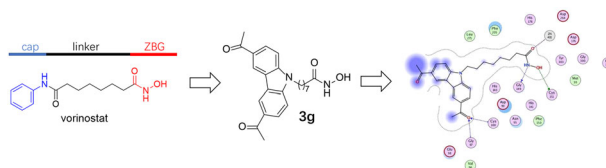
Received: 22 February 2023 / Accepted: 16 May 2023 / Published online: 2 June 2023

© The Author(s), under exclusive licence to Springer Science+Business Media, LLC, part of Springer Nature 2023

Abstract

Histone deacetylase (HDAC), a key regulator in controlling the acetylation status of histone, are considered to be associated with viability, migration, invasion, proliferation and apoptosis of malignant tumors. The HDAC inhibition is an effective strategy for designing compounds against malignant tumors and five compounds have been approved by FDA or NMPA for clinical therapy. In this study, we designed and synthesized a series of novel carbazole-hydroxamate analogues as HDAC inhibitors and evaluated their anti-tumor properties *in vitro*. Compared with vorinostat, the HDAC semi-inhibitory concentration of compounds **3f** and **3g** decreased 4–13 folds, compounds **8a** and **8c** also showed strong inhibitory HDAC activity, and compound **3g** had a strong inhibitory effect on HDAC 1. The CCK8 assay showed that compounds **3g** displayed good antiproliferative activity on tested tumor cells. Flow cytometric and western blot assay showed that **3g** exerted anti-tumor activities by regulating the level of Ac-HH3 and activating the cleaved caspase 3. Based on these results, carbazole-hydroxamate derivative **3g** might become a potential anti-tumor candidate molecule to further structural optimization research.

Graphical Abstract



Keywords Carbazole · HDAC inhibitory · Antitumor · Apoptosis

Supplementary information The online version contains supplementary material available at <https://doi.org/10.1007/s00044-023-03084-0>.

- ✉ Chen Chen
chenlwchen@163.com
- ✉ Chengyun Zheng
sdeyzcy@email.sdu.edu.cn

¹ Department of Hematology, The Second Hospital of Shandong University, Jinan, Shandong Province, China

² Department of Medicine, The Second Hospital of Shandong University, Jinan, Shandong Province, China

³ School of Pharmaceutical Sciences, Qilu University of Technology (Shandong Academy of Sciences), Jinan, Shandong Province, China

Introduction

Histone deacetylases (HDACs) and histone acetyltransferases (HATs) are crucial regulators which controlled the acetylation status of histones [1, 2]. HDACs, especially class I isozymes (1, 2, 3, and 8) are considered to be associated with the progression of tumorigenesis such as malignancies viability, migration, invasion, proliferation, as well as the induction of cell apoptosis [3–6]. The HDAC inhibition strategy have been proved to be effective for tumor therapy against malignant tumors and five compounds (vorinostat, romidepsin, belinostat, panobinostat, and chidamide) have been approved by FDA or CFDA for clinical therapy [7] (Fig. 1).

Fig. 1 Marketed HDAC inhibitors

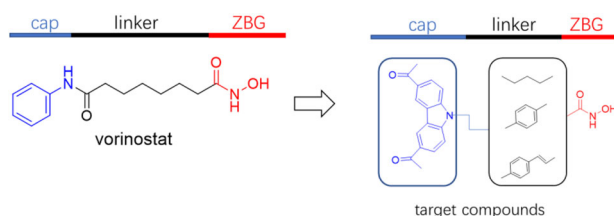
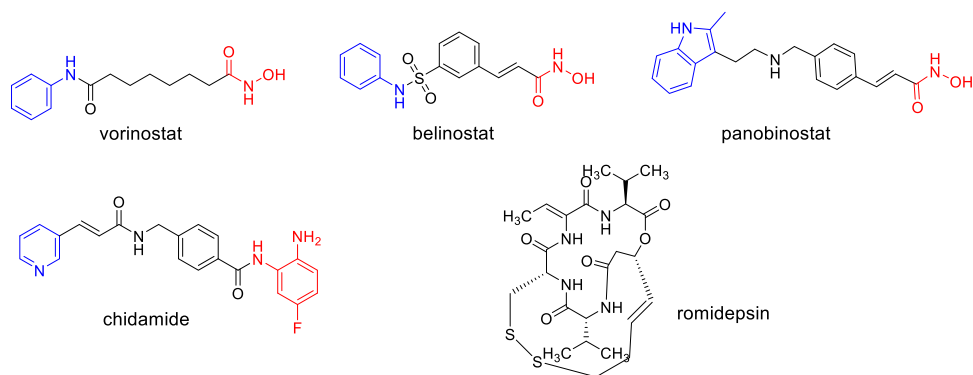


Fig. 2 Design strategy of target compounds

The common HDAC inhibitors, like SAHA (vorinostat) and belinostat, fit a three-motif pharmacophoric model, comprising of a cap group, a linker and a zinc-binding group (ZBG) [8, 9]. The cap groups are crucial for identifying the surface of protein and the appropriate linkers are benefit for ZBG entering the active pocket and chelating Zn^{2+} [10]. Thus, exploring new cap groups and appropriate linkers might afford more stronger inhibitors.

Carbazole, an aromatic heterocyclic compound, originated from the murrayanine since 1962. Thereafter, a number of carbazole derivatives were synthesized and exerted diverse biological activities, such as anticancer, anti-inflammation, anti-Alzheimer and pro-apoptosis [11–13]. Following our previous design experience in HDAC inhibitors [14–16], substituted carbazoles were introduced as the cap groups and diverse linkers were used to connect cap groups to hydroxamate group (Fig. 2). A series of carbazole-hydroxamate derivatives were synthesized and evaluated their biological activities in this article. After biological characterizations, including HeLa nuclear extract activity, HDAC isozymes activity, pro-apoptotic activity, **3g** was identified as the most potent compound. It exhibited several striking characteristics: 5.9 nM HDAC1 inhibition activity; micromolar antiproliferative activity on tested tumor cell lines equivalent to SAHA; obvious apoptosis-inducing effect. These results disclosed that **3g** was a promising lead compound for further structural optimization.

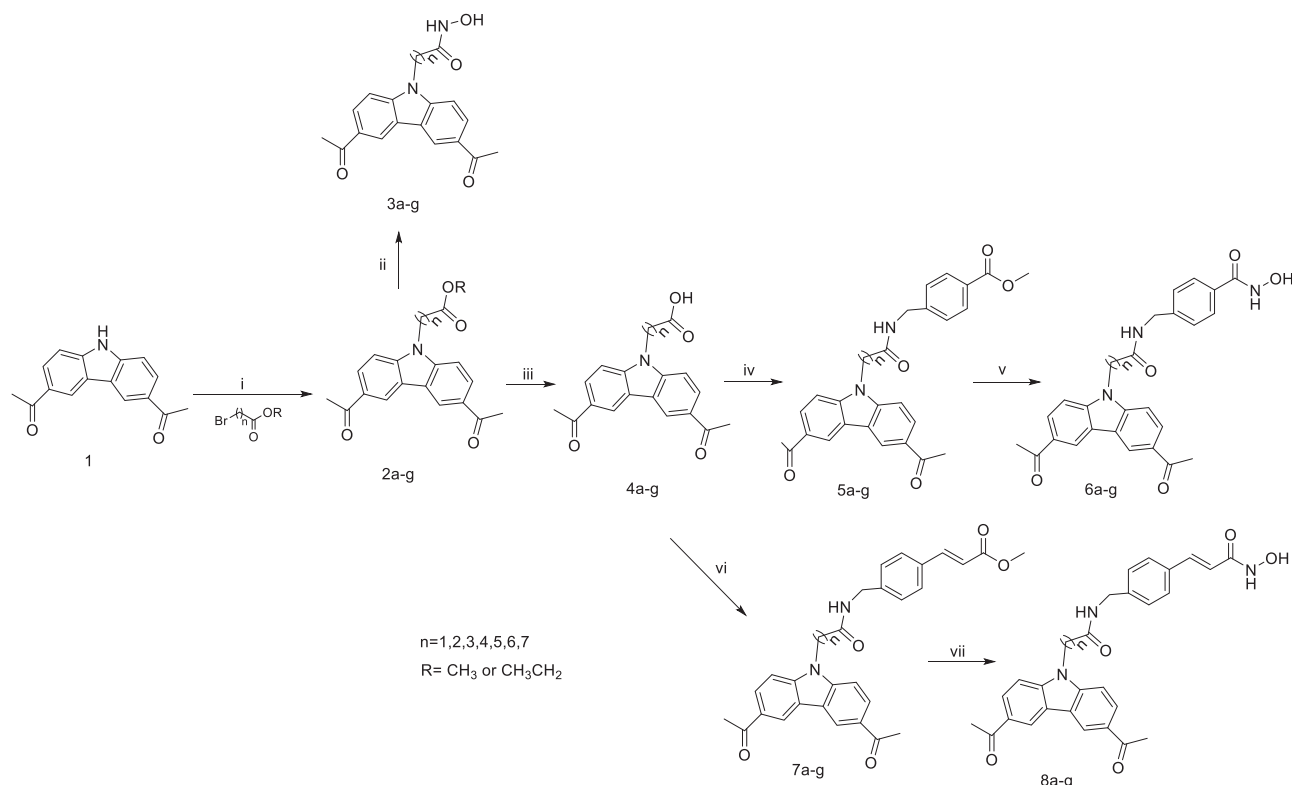
Results and discussion

Chemistry

The reaction routes of all target compounds were described in Scheme 1. Starting material 1,1'-(9H-carbazole-3,6-diyl)diethanone (**1**) was synthesized according to the previous report [17]. Starting from compound **1**, carbazole derivatives **2a-g** was obtained by nucleophilic substitution. The **2a-g** were coupled with NH_2OH to form the target compounds **3a-g**. Removal of ester group to carboxylic acid in **2a-g** using NaOH in THF/ H_2O solution yielded compounds **4a-g**. Compound **4a-g** were subjected to amidation coupling reaction with methyl 4-(aminomethyl)cinnamate and methyl 4-(aminomethyl)benzoate to afford **5a-g** or **7a-g**, followed by coupling with NH_2OH formed the target compounds **6a-g** or **8a-g**.

HeLa cell extract activity

HeLa cell extract activity assay was usually applied to evaluate preliminary HDAC inhibitory activity of target compounds [15]. All compounds were screened for HeLa cell extract activities at 1000 nM, and compounds **3f**, **3g**, **6a**, **6b**, **6c**, **6f**, **8a**, **8c**, **8d**, **8e**, **8f**, **8g** with inhibition rates higher than 50% were further tested to determine IC_{50} values (Table 1). Initially, the effects of linker length on HeLa cell extract activity was investigated. For compounds **3a-g** with increasing $-CH_2-$ units in structure, the **3f** and **3g** with linker bearing six and seven $-CH_2-$ units showed the best inhibition potent (14 ± 0.5 nM, 5.3 ± 1.2 nM, respectively). Compared with SAHA, the IC_{50} values of **3f** and **3g** decreased 4–13 folds. Next, N-OH-benzamide or N-OH-cinnamide were introduced to substitute for hydroxamic acid to afford **6a-g** and **8a-g**. The introduction of N-OH-benzamide or N-OH-cinnamide seemed to be benefit for inhibition and most of compounds possessed good inhibition potent with IC_{50} values lower than 1000 nM. The best active compounds **8a** and **8c** respectively displayed the 23.5 nM and 66.8 nM inhibitory activities relative to 67.7 nM of SAHA.



Scheme 1 Reagents and conditions: (i) K_2CO_3 , DMF, $80^\circ C$, 4–6 h; (ii) $NH_2OH \cdot HCl$, KOH, MeOH, rt, 1 h; (iii) NaOH, MeOH, H_2O , reflux, 1–2 h; (iv) Methyl 4-(aminomethyl)benzoate, TBTU, DIEA,

DCM, rt, 8 h; (v) $NH_2OH \cdot HCl$, KOH, MeOH, rt, 1 h; (vi) TBTU, DIEA, DCM, rt, 8 h; (vii) $NH_2OH \cdot HCl$, KOH, MeOH, rt, 1 h

HDAC isoforms inhibitory activity of selected compounds HDAC

Compounds **3f**, **3g**, **8a**, and **8c** with stronger inhibition potency relative to SAHA were selected to evaluate their inhibitory effects on HDAC isoform enzymes 1, 6, and 8. As shown in Table 2, these compounds were more sensitive to HDAC1 than HDAC6 and HDAC8. Compound **3g** exhibited the best inhibition effects on HDAC1 with IC_{50} value of 5.9 nM, an increase of 10 folds than that of SAHA. Compounds **3f**, **8a**, and **8c** showed similar inhibition against HDAC1. For HDAC6, these compounds all displayed weak inhibition activities than SAHA. For HDAC8, only compound **3f** increased 2-folds inhibitory activities relative to SAHA. Taken together, the compound **3g** possess potent inhibition against HDAC1 and a degree of selectivity for HDAC1 over HDAC6 and HDAC8 (27-folds and 1206-folds).

In vitro antiproliferative activity

Compounds **3f**, **3g**, **8a**, and **8c** were subsequently selected to evaluate their antiproliferative activities against HCT116, HepG2, HeLa, HEL, Molt4, and U266 cell lines, with SAHA as positive control (Table 3). In terms of the inhibition influence on HCT116 and HepG2 cells,

compound **3f** and **3g** showed higher inhibition, whereas the IC_{50} values of **8a** and **8c** exceeded $25 \mu M$. For HeLa cells, compounds **3g** and **8c** showed a degree of inhibition. Against the hematologic tumor cells (HEL and Molt4), **3g** and **8c** exhibited much stronger antiproliferative activities than **3f** and **8a**. Above all, these compounds possessed different antiproliferative activities to different cancer cells.

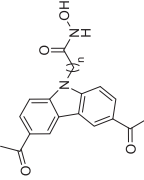
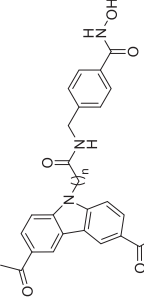
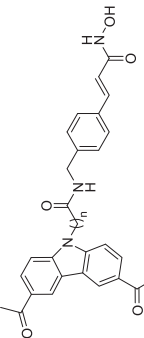
Cell apoptosis assay

Afterward, we tested the pro-apoptosis effect of compound **3g** on Molt4 cells after 24 h co-incubation. Compared with the control (3.79%) and SAHA (15.58%), compound **3g** induced 24.46% and 48.50% Molt4 cell apoptosis at 0.5 and $1.5 \mu M$. These results confirmed its notable pro-apoptosis activity on Molt4 cells (Fig. 3).

Western blot assay

Western blot assay was performed to test compound **3g** influence on the acetylation of histone h3 (Ac-HH3), acetylation of tubulin (Ac-Tubulin) and cleaved caspase 3. As shown in Fig. 4, compound **3g** enhanced the acetylation of histone h3 at the concentration of $1.5 \mu M$, much stronger than SAHA on the acetylation-induced capacity at the same concentration. For

Table 1 The chemical structures and HeLa cell extract activity

Cpd.	<i>n</i>	IC ₅₀ ^a (nM)	Cpd.	<i>n</i>	IC ₅₀ ^a (nM)	Cpd.	<i>n</i>	IC ₅₀ ^a (nM)
	1	>1000		1	416 ± 26		1	23.5 ± 0.9
3b	2	>1000	6b	2	323 ± 42	8b	2	>1000
3c	3	>1000	6c	3	114 ± 11	8c	3	66.8 ± 4.2
3d	4	>1000	6d	4	>1000	8d	4	146 ± 11
3e	5	>1000	6e	5	>1000	8e	5	184 ± 5
3f	6	14 ± 0.5	6f	6	391 ± 34	8f	6	144 ± 2
3g	7	5.3 ± 1.2	6g	7	>1000	8g	7	292 ± 20
SAHA		67.7 ± 2.5						

^aEach compound was tested in triplicate; the data are presented as the mean ± SEM (*n* = 3)

Table 2 HDAC isoforms inhibitory activity

Cpd.	IC ₅₀ ^a (nM)		
	HDAC1	HDAC6	HDAC8
3f	32.5 ± 4.1	77.4 ± 2.2	2271 ± 48
3g	5.9 ± 0.4	160 ± 17	7116 ± 106
8a	78.7 ± 2.0	632 ± 7	>20,000
8c	60.8 ± 10.8	666 ± 50	8056 ± 153
SAHA	52 ± 2	22.9 ± 2.4	4379 ± 31

^aEach compound was tested in triplicate; the data are presented as the mean ± SEM (*n* = 3)

acetylation of tubulin, compound **3g** didn't displayed significant acetylation-induced capacity at the concentration of 1.5 μM, whereas SAHA obviously increased the acetylation of tubulin. These results indicated that compound **3g** had a more significant inhibitory effect on HDAC1 than on HDAC6, which agreed with the results in the HDAC isoforms inhibitory activity. Besides, **3g** induced the cleavage of caspase-3, which indicated the activation of apoptosis.

Molecular docking study

Molecular docking was performed to investigate the interactions between **3g** with HDAC1 protein (PDB code: 5ICN). As shown in Fig. 5A, B, the carbazole core occupied the outer surface of HDAC1 catalytic pocket and forms key interactions with Gly97 and Cys100. The fatty chain linkers and hydroxamic acids extended to the catalytic pocket around Zn²⁺. The carbonyl group chelated with zinc ions. Furthermore, the hydroxyl and amino groups interacted with Cys151 and Gly149 through hydrogen bond interactions. The docking of SAHA with HDAC1 was also performed and the result was as shown in Fig. 5C, D. Similar to **3g**, the O of carbonyl chelated with Zn401 and the hydroxyl and amino groups interacted with Cys151 and Gly149. These results explained why the inhibition activity of **3g** was similar to SAHA.

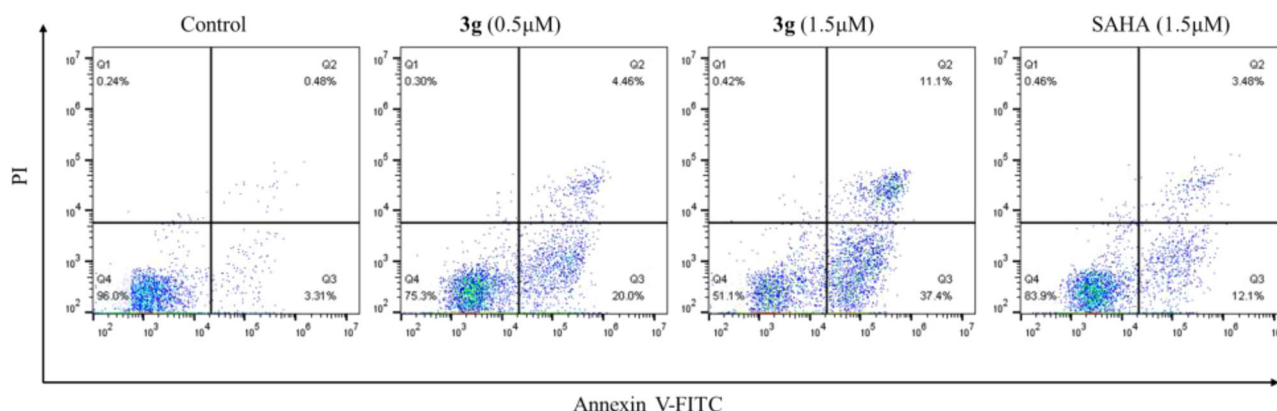
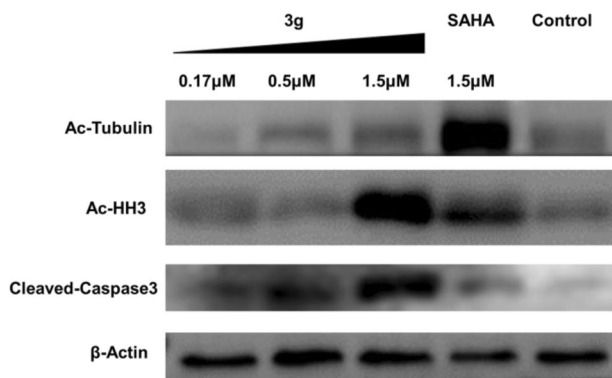
Conclusion

In this study, a series of novel carbazole-hydroxamate analogues were designed and synthesized as HDAC inhibitors. Through screening, compound **3g** displayed potent enzyme and tumor cells inhibition activities. Flow cytometry and western blot assay showed that compound **3g** could efficiently induce apoptosis through caspase-3 pathway. Western blot assay also revealed that compound **3g** possessed stronger histone h3 acetylation-induced capacity, consistent with its stronger HDAC1 inhibitory activity. Based on these results, carbazole-hydroxamate derivative **3g** might become a potential anti-tumor candidate molecule to further structural optimization research.

Table 3 Antiproliferative activity

Cpd.	IC ₅₀ ^a (μ M)						
	HCT116	HepG2	Hela	HEL	Molt4	U266	293t
3f	4.0 \pm 0.21	10 \pm 0.96	>25	>25	13 \pm 2.2	6.0 \pm 0.57	>100
3g	2.2 \pm 0.23	12 \pm 0.09	17 \pm 0.47	3.5 \pm 0.37	0.45 \pm 0.02	3.9 \pm 0.13	>100
8a	>25	>25	>25	18 \pm 2.1	3.3 \pm 0.06	2.1 \pm 0.20	>100
8c	>25	>25	10 \pm 0.90	2.1 \pm 0.09	1.2 \pm 0.09	4.2 \pm 0.49	>100
SAHA	2.3 \pm 0.01	18 \pm 1.4	3.8 \pm 0.33	0.50 \pm 0.01	0.61 \pm 0.09	0.33 \pm 0.02	–

^aEach compound was tested in triplicate; the data are presented as the mean \pm SEM ($n = 3$)

**Fig. 3** The pro-apoptosis effect of compound **3g** on Molt4 cells**Fig. 4** Western blot analysis of Ac-HH3, Ac- α -tubulin and cleaved-caspase3 in Molt4 cells after 24 h treatment

Experimental

General synthesis of compounds

Reagents and solvents used were of commercially available and without further purification. Melting points were recorded by the electrothermal melting point apparatus. ¹H and ¹³C NMR spectra were recorded on a Bruker DRX spectrometer at 400 MHz. High-resolution mass spectra (HRMS) were conducted on an Agilent 6510 Quadrupole Time-of-Flight LC/MS deliver.

ethyl 2-(3,6-diacetyl-9H-carbazol-9-yl)acetate (**2a**)

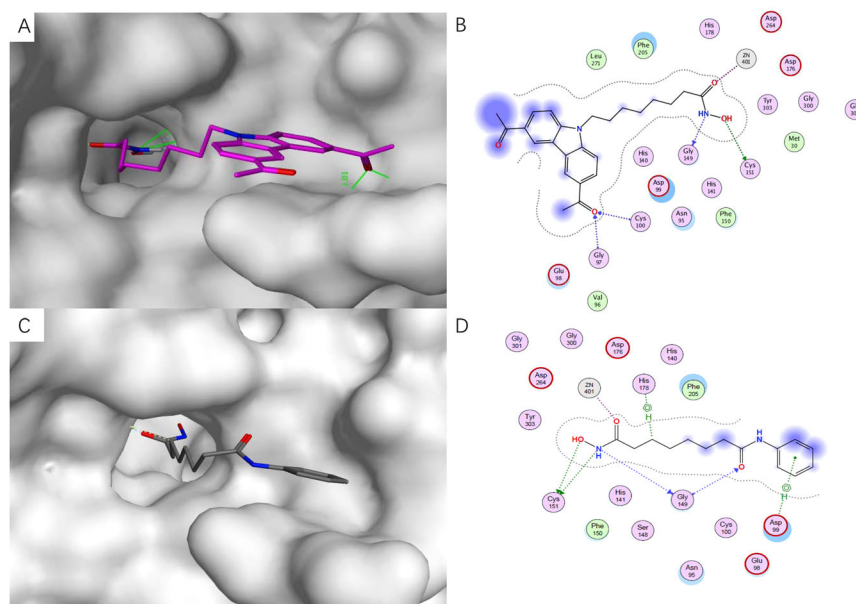
1,1'-(9H-carbazole-3,6-diyl)diethanone (0.76 g, 3.0 mmol, 1.0 eq) was dissolved in a mixture of DMF (5.0 mL) and K₂CO₃ (0.84 g, 6.0 mmol, 2.0 eq). Then the ethyl bromoacetate (0.60 g, 3.6 mmol, 1.2 eq) was added and heated to 80 °C for 4–6 h. After that, 25 mL H₂O was added into the mixture. The mixture was extracted by EtOAc (\times 3). Later, the EtOAc layer was washed by saturated brine solution, dried with anhydrous MgSO₄, filtered and reduced to yield an light yellow solid. The crude residue was further purified by flash column chromatography on a silica gel using CH₂Cl₂/CH₃OH (100:1), yield 74%. Mp: 202–203 °C. ¹H NMR (400 MHz, Chloroform-*d*) δ 8.81 (d, $J = 1.8$ Hz, 2H), 8.19 (dd, $J = 8.7, 1.7$ Hz, 2H), 7.40 (d, $J = 8.6$ Hz, 2H), 5.07 (s, 2H), 4.23 (q, $J = 7.1$ Hz, 2H), 2.75 (s, 6H), 1.25 (t, $J = 7.2$ Hz, 3H).

2b-2g were synthesized in the same way as **2a**.

methyl 3-(3,6-diacetyl-9H-carbazol-9-yl)propanoate (**2b**)

White solid. Mp: 158–160 °C. ¹H NMR (400 MHz, Chloroform-*d*) δ 8.81 (d, $J = 1.8$ Hz, 2H), 8.19 (dd, $J = 8.7, 1.7$ Hz, 2H), 7.43 (d, $J = 8.7$ Hz, 2H), 4.43 (q, $J = 7.1$ Hz, 2H), 3.72 (s, 3H), 2.75 (s, 6H), 2.25 (t, $J = 7.2$ Hz, 2H).

Fig. 5 Molecular docking mode of **3g** (**A**, **B**) and SAHA (**C**, **D**) with HDAC1 protein (PDB code: 5ICN)



methyl 4-(3,6-diacetyl-9H-carbazol-9-yl)butanoate (2c)

White solid. Mp: 146–147 °C. ^1H NMR (400 MHz, Chloroform-*d*) δ 8.80 (d, $J = 1.7$ Hz, 2H), 8.19 (dd, $J = 8.7$, 1.7 Hz, 2H), 7.50 (d, $J = 8.7$ Hz, 2H), 4.47 (t, $J = 7.2$ Hz, 2H), 3.69 (s, 3H), 2.75 (s, 6H), 2.38 (t, $J = 6.8$ Hz, 2H), 2.29–2.18 (m, 2H).

ethyl 5-(3,6-diacetyl-9H-carbazol-9-yl)pentanoate (2d)

White solid. Mp: 145–146 °C. ^1H NMR (400 MHz, Chloroform-*d*) δ 8.80 (d, $J = 1.8$ Hz, 2H), 8.19 (dd, $J = 8.7$, 1.7 Hz, 2H), 7.47 (d, $J = 8.7$ Hz, 2H), 4.39 (t, $J = 7.2$ Hz, 2H), 4.10 (q, $J = 7.2$ Hz, 2H), 2.75 (s, 6H), 2.33 (t, $J = 7.2$ Hz, 2H), 1.95 (q, $J = 7.6$ Hz, 2H), 1.73 (q, $J = 7.6$ Hz, 2H), 1.21 (t, $J = 7.2$ Hz, 3H).

methyl 6-(3,6-diacetyl-9H-carbazol-9-yl)hexanoate (2e)

White solid. Mp: 140–141 °C. ^1H NMR (400 MHz, Chloroform-*d*) δ 8.80 (d, $J = 1.8$ Hz, 2H), 8.18 (dd, $J = 8.7$, 1.8 Hz, 2H), 7.46 (d, $J = 8.7$ Hz, 2H), 4.37 (t, $J = 7.2$ Hz, 2H), 3.64 (s, 3H), 2.75 (s, 6H), 2.29 (t, $J = 7.3$ Hz, 2H), 1.93 (p, $J = 7.4$ Hz, 2H), 1.68 (p, $J = 7.4$ Hz, 2H), 1.42 (tt, $J = 9.7$, 6.2 Hz, 2H).

ethyl 7-(3,6-diacetyl-9H-carbazol-9-yl)heptanoate (2f)

White solid. Mp: 110–111 °C. ^1H NMR (400 MHz, Chloroform-*d*) δ 8.80 (d, $J = 1.8$ Hz, 2H), 8.18 (dd, $J = 8.7$, 1.7 Hz, 2H), 7.46 (d, $J = 8.7$ Hz, 2H), 4.36 (t, $J = 7.2$ Hz, 2H), 4.10 (q, $J = 7.2$ Hz, 2H), 2.75 (d, $J = 2.5$ Hz, 6H), 2.26 (t, $J = 7.4$ Hz, 2H), 1.91 (t, $J = 7.2$ Hz, 2H), 1.60

(d, $J = 6.5$ Hz, 2H), 1.39 (dd, $J = 7.3$, 3.5 Hz, 4H), 1.23 (t, $J = 7.2$ Hz, 3H).

ethyl 8-(3,6-diacetyl-9H-carbazol-9-yl)octanoate (2g)

White solid. Mp: 95–96 °C. ^1H NMR (400 MHz, Chloroform-*d*) δ 8.84 (d, $J = 1.8$ Hz, 2H), 8.28 (dd, $J = 8.7$, 1.7 Hz, 2H), 7.35 (d, $J = 8.7$ Hz, 2H), 4.32 (t, $J = 7.2$ Hz, 2H), 3.75 (m, 2H), 2.73 (s, 6H), 2.32 (t, $J = 7.4$ Hz, 2H), 1.91 (t, $J = 6.6$ Hz, 2H), 1.54 (t, $J = 7.3$ Hz, 2H), 1.40–1.22 (m, 9H).

2-(3,6-diacetyl-9H-carbazol-9-yl)-N-hydroxyacetamide (3a)

The synthesis method was according to our previous published article [16]. Yield 49%. Light yellow solid. Mp: 202–203 °C. ^1H NMR (400 MHz, DMSO-*d*₆) δ 8.48 (d, $J = 1.8$ Hz, 2H), 7.83 (dd, $J = 8.7$, 1.8 Hz, 2H), 7.55 (d, $J = 8.8$ Hz, 2H), 5.23 (s, 2H), 2.30 (s, 6H). ^{13}C NMR (101 MHz, DMSO) δ 170.47, 153.92, 141.53, 129.26, 124.06, 122.77, 118.53, 109.89, 44.71, 12.42. HRMS (ESI) m/z Calcd $[\text{M} + \text{H}]^+$ 325.1183, found: 325.1184.

3b–3g were synthesized in the same way as **3a**.

3-(3,6-diacetyl-9H-carbazol-9-yl)-N-hydroxypropanamide (3b)

White solid. Mp: 213–215 °C. ^1H NMR (400 MHz, DMSO-*d*₆) δ 8.47 (d, $J = 1.8$ Hz, 2H), 7.85 (dd, $J = 8.7$, 1.8 Hz, 2H), 7.63 (d, $J = 8.7$ Hz, 2H), 4.64 (t, $J = 7.1$ Hz, 2H), 2.75 (t, $J = 7.0$ Hz, 2H), 2.30 (s, 6H). ^{13}C NMR (101 MHz, DMSO) δ 173.05, 153.89, 140.72, 128.99, 124.00, 122.70, 118.54, 110.02, 34.14, 12.38. HRMS (ESI) m/z Calcd $[\text{M} + \text{H}]^+$ 337.1194, found: 337.1197.

4-(3,6-diacetyl-9H-carbazol-9-yl)-N-hydroxybutanamide (3c)

White solid. Mp: 175–177 °C. ^1H NMR (400 MHz, DMSO- d_6) δ 8.48 (s, 2H), 7.86 (dd, $J = 8.7, 1.8$ Hz, 2H), 7.62 (d, $J = 8.8$ Hz, 2H), 4.43 (d, $J = 7.3$ Hz, 2H), 2.30 (s, 6H), 2.06–1.94 (m, 4H). ^{13}C NMR (101 MHz, DMSO) δ 168.98, 153.91, 140.95, 128.88, 124.02, 122.58, 118.65, 109.81, 42.47, 29.69, 25.05, 12.39. HRMS (ESI) m/z Calcd $[\text{M} + \text{H}]^+$ 353.1496, found: 353.1499.

5-(3,6-diacetyl-9H-carbazol-9-yl)-N-hydroxypentanamide (3d)

White solid. Mp: 191–192 °C. ^1H NMR (400 MHz, DMSO- d_6) δ 8.47 (s, 2H), 7.88–7.82 (m, 2H), 7.61 (d, $J = 8.7$ Hz, 2H), 4.42 (t, $J = 7.0$ Hz, 2H), 2.30 (s, 6H), 2.22 (t, $J = 7.4$ Hz, 2H), 1.82–1.75 (m, 2H), 1.51 (t, $J = 7.8$ Hz, 2H). ^{13}C NMR (101 MHz, DMSO) δ 197.51, 174.78, 153.91, 140.98, 128.80, 123.98, 122.54, 118.61, 109.85, 42.70, 33.95, 28.61, 22.60, 12.37. HRMS (ESI) m/z Calcd $[\text{M} + \text{H}]^+$ 367.1652, found: 367.1656.

6-(3,6-diacetyl-9H-carbazol-9-yl)-N-hydroxyhexanamide (3e)

White solid. Mp: 161–163 °C. ^1H NMR (400 MHz, DMSO- d_6) δ 8.46 (s, 2H), 7.85 (dd, $J = 8.7, 1.8$ Hz, 2H), 7.58 (d, $J = 8.7$ Hz, 2H), 4.37 (t, $J = 7.2$ Hz, 2H), 2.30 (s, 6H), 1.84 (t, $J = 7.3$ Hz, 2H), 1.75 (t, $J = 7.5$ Hz, 2H), 1.55–1.40 (m, 2H), 1.33–1.20 (m, 2H). ^{13}C NMR (101 MHz, DMSO) δ 178.17, 153.79, 140.96, 128.78, 123.98, 122.51, 118.55, 109.77, 43.03, 38.38, 29.12, 27.27, 26.55, 12.36. HRMS (ESI) m/z Calcd $[\text{M} + \text{H}]^+$ 379.1663, found: 379.1668.

7-(3,6-diacetyl-9H-carbazol-9-yl)-N-hydroxyheptanamide (3f)

White solid. Mp: 171–173 °C. ^1H NMR (400 MHz, DMSO- d_6) δ 10.32 (s, 1H), 8.64 (s, 1H), 8.50–8.43 (m, 2H), 7.91–7.82 (m, 2H), 7.61 (dd, $J = 8.9, 5.4$ Hz, 2H), 4.40 (d, $J = 6.7$ Hz, 2H), 2.30 (s, 6H), 1.89 (t, $J = 6.9$ Hz, 2H), 1.77 (q, $J = 7.4, 7.0$ Hz, 2H), 1.43 (q, $J = 6.9$ Hz, 2H), 1.38–1.20 (m, 4H). ^{13}C NMR (101 MHz, DMSO) δ 169.54, 153.91, 140.98, 128.77, 123.99, 122.53, 118.63, 109.82, 42.89, 32.64, 28.90, 28.76, 26.60, 25.44, 12.38. HRMS (ESI) m/z Calcd $[\text{M} + \text{H}]^+$ 395.1965, found: 395.1968.

8-(3,6-diacetyl-9H-carbazol-9-yl)-N-hydroxyoctanamide (3g)

White solid. Mp: 171–172 °C. ^1H NMR (400 MHz, DMSO- d_6) δ 10.31 (s, 1H), 8.64 (s, 1H), 8.47 (d, $J = 1.9$ Hz, 2H),

7.86 (dd, $J = 8.7, 1.8$ Hz, 2H), 7.60 (d, $J = 8.7$ Hz, 2H), 4.40 (t, $J = 7.0$ Hz, 2H), 2.30 (s, 6H), 1.89 (t, $J = 7.4$ Hz, 2H), 1.82–1.71 (m, 2H), 1.42 (q, $J = 7.5$ Hz, 2H), 1.27 (d, $J = 6.1$ Hz, 4H), 1.20–1.08 (m, 2H). ^{13}C NMR (101 MHz, DMSO) δ 169.57, 153.92, 140.99, 128.76, 123.98, 122.53, 118.62, 109.84, 42.91, 32.66, 29.05, 28.98, 28.95, 26.85, 25.51, 12.38. HRMS (ESI) m/z Calcd $[\text{M} + \text{H}]^+$ 409.2122, found: 409.2124.

2-(3,6-diacetyl-9H-carbazol-9-yl)acetic acid (4a)

Compound **2a** (0.68 g, 2.0 mmol, 1.0eq) was dissolved in MeOH (6 mL), then the solution of NaOH (1 M, 6 mL) was added. The mixture was stirred at reflux for 4 h. Then the mixture was neutralized with 1 M HCl to PH 2-3. White precipitate obtained was filtered and vacuum drying. Yield 63%. Light yellow solid. Mp: 289–290 °C. ^1H NMR (400 MHz, Chloroform- d) δ 8.78 (d, $J = 1.8$ Hz, 2H), 8.19 (dd, $J = 8.7, 1.7$ Hz, 2H), 7.43 (d, $J = 8.6$ Hz, 2H), 5.01 (s, 2H), 2.74 (s, 6H).

4b-4g were synthesized in the same way as **4a**.

3-(3,6-diacetyl-9H-carbazol-9-yl)propanoic acid (4b)

Light yellow solid. Mp: 191–192 °C. ^1H NMR (400 MHz, Chloroform- d) δ 8.81 (d, $J = 1.8$ Hz, 2H), 8.19 (dd, $J = 8.7, 1.7$ Hz, 2H), 7.43 (d, $J = 8.7$ Hz, 2H), 4.43 (q, $J = 7.1$ Hz, 2H), 3.72 (s, 3H), 2.75 (s, 6H), 2.25 (t, $J = 7.2$ Hz, 2H).

4-(3,6-diacetyl-9H-carbazol-9-yl)butanoic acid (4c)

Light yellow solid. Mp: 220–221 °C. ^1H NMR (400 MHz, Chloroform- d) δ 8.74 (d, $J = 1.8$ Hz, 2H), 8.13 (d, $J = 8.7$ Hz, 2H), 7.44 (d, $J = 8.7$ Hz, 2H), 4.42 (t, $J = 6.8$ Hz, 2H), 2.68 (s, 6H), 2.38 (t, $J = 6.8$ Hz, 2H).

5-(3,6-diacetyl-9H-carbazol-9-yl)pentanoic acid (4d)

Light yellow solid. Mp: 215–216 °C. ^1H NMR (400 MHz, Chloroform- d) δ 8.80 (d, $J = 1.8$ Hz, 2H), 8.19 (dd, $J = 8.7, 1.7$ Hz, 2H), 7.47 (d, $J = 8.7$ Hz, 2H), 4.39 (t, $J = 7.2$ Hz, 2H), 3.90 (q, $J = 7.2$ Hz, 2H), 2.75 (s, 6H), 2.33 (t, $J = 7.2$ Hz, 2H), 1.95 (q, $J = 7.6$ Hz, 2H).

6-(3,6-diacetyl-9H-carbazol-9-yl)hexanoic acid (4e)

Light yellow solid. Mp: 155–156 °C. ^1H NMR (400 MHz, Chloroform- d) δ 8.80 (d, $J = 1.8$ Hz, 2H), 8.18 (dd, $J = 8.7, 1.8$ Hz, 2H), 7.46 (d, $J = 8.7$ Hz, 2H), 4.37 (t, $J = 7.2$ Hz, 2H), 2.75 (s, 6H), 2.29 (t, $J = 7.3$ Hz, 2H), 1.93 (p, $J = 7.4$ Hz, 2H), 1.68 (p, $J = 7.4$ Hz, 2H), 1.42 (tt, $J = 9.7, 6.2$ Hz, 2H).

7-(3,6-diacetyl-9H-carbazol-9-yl)heptanoic acid (4f)

Light yellow solid. Mp:175–176 °C. ^1H NMR (400 MHz, Chloroform-*d*) δ 8.80 (d, $J = 1.8$ Hz, 2H), 8.18 (dd, $J = 8.7$, 1.7 Hz, 2H), 7.46 (d, $J = 8.7$ Hz, 2H), 4.36 (t, $J = 7.2$ Hz, 2H), 2.75 (s, 6H), 2.26 (t, $J = 7.4$ Hz, 2H), 1.91 (t, $J = 7.2$ Hz, 2H), 1.60 (d, $J = 6.5$ Hz, 2H), 1.39 (dd, $J = 7.3$, 3.5 Hz, 4H).

8-(3,6-diacetyl-9H-carbazol-9-yl)octanoic acid (4g)

Light yellow solid. Mp:155–156 °C. ^1H NMR (400 MHz, Chloroform-*d*) δ 8.79 (d, $J = 1.8$ Hz, 2H), 8.18 (dd, $J = 8.7$, 1.7 Hz, 2H), 7.45 (d, $J = 8.7$ Hz, 2H), 4.35 (t, $J = 7.2$ Hz, 2H), 2.75 (s, 6H), 2.30 (t, $J = 7.4$ Hz, 2H), 1.90 (t, $J = 6.6$ Hz, 2H), 1.58 (t, $J = 7.3$ Hz, 2H), 1.44 – 1.21 (m, 6H).

methyl 4-((2-(3,6-diacetyl-9H-carbazol-9-yl)acetamido)methyl)benzoate (5a)

Compound **4a** (0.31 g, 1.0 mmol, 1.0eq) was dissolved in 20 mL DCM, TBTU (0.39 g, 1.2 mmol, 1.2eq) and DIEA (0.39 g, 3 mmol, 3eq) was added. After stirring 0.5 h, methyl 4-(aminomethyl)benzoate (0.26 g, 1.1 mmol, 1.1eq) was added and the reaction was stirred at RT for 8–10 h. Then the mixture was washed with 1 M citric acid ($\times 3$), saturate solution of NaHCO_3 ($\times 3$) and brine solution ($\times 3$). The organic layer was concentrated in vacuo, then purified via chromatography on silica (DCM/MeOH 80:1) to give a white solid as the target compound. Yield 67%. Mp:274–275 °C. ^1H NMR (400 MHz, Chloroform-*d*) δ 8.74 (d, $J = 1.7$ Hz, 2H), 8.17 (dd, $J = 8.6$, 1.7 Hz, 2H), 7.88 (d, $J = 8.2$ Hz, 2H), 7.44 (d, $J = 8.6$ Hz, 2H), 7.13 (d, $J = 8.0$ Hz, 2H), 6.04 (d, $J = 6.6$ Hz, 1H), 5.07 (s, 2H), 4.45 (d, $J = 6.1$ Hz, 2H), 3.87 (s, 3H), 2.70 (s, 6H). **5b–5g** were synthesized in the same way as **5a**.

Ethyl 4-((3-(3,6-diacetyl-9H-carbazol-9-yl)propanamido)methyl)benzoate (5b)

White solid. Mp:207–208 °C. ^1H NMR (400 MHz, Chloroform-*d*) δ 8.77 (d, $J = 1.7$ Hz, 2H), 8.13 (dd, $J = 8.7$, 1.7 Hz, 2H), 7.87–7.70 (m, 2H), 7.54 (d, $J = 8.6$ Hz, 2H), 6.91 (d, $J = 8.0$ Hz, 2H), 5.74 (s, 1H), 4.80 (t, $J = 6.3$ Hz, 2H), 4.31 (d, $J = 5.9$ Hz, 2H), 3.89 (s, 3H), 2.80 (q, $J = 4.3$, 2.5 Hz, 2H), 2.73 (s, 6H).

Methyl 4-((4-(3,6-diacetyl-9H-carbazol-9-yl)butanamido)methyl)benzoate (5c)

White solid. Mp:195–196 °C. ^1H NMR (400 MHz, Chloroform-*d*) δ 8.78 (d, $J = 1.6$ Hz, 2H), 8.13

(dd, $J = 8.7$, 1.7 Hz, 2H), 8.00 (d, $J = 8.1$ Hz, 2H), 7.49 (d, $J = 8.7$ Hz, 2H), 7.32 (d, $J = 8.0$ Hz, 2H), 5.69 (s, 1H), 4.56–4.47 (m, 4H), 3.91 (s, 3H), 2.73 (s, 6H), 2.30 (p, $J = 6.6$ Hz, 2H), 2.27–2.20 (m, 2H).

Methyl 4-((5-(3,6-diacetyl-9H-carbazol-9-yl)pentanamido)methyl)benzoate (5d)

White solid. Mp:207–208 °C. ^1H NMR (400 MHz, Chloroform-*d*) δ 8.80 (d, $J = 1.7$ Hz, 2H), 8.18 (dd, $J = 8.6$, 1.7 Hz, 2H), 7.95 (d, $J = 8.2$ Hz, 2H), 7.47 (d, $J = 8.6$ Hz, 2H), 7.28 (d, 2H), 4.45 (d, $J = 5.9$ Hz, 2H), 4.41 (t, $J = 7.0$ Hz, 2H), 3.91 (s, 3H), 2.75 (s, 6H), 2.23 (t, $J = 7.2$ Hz, 2H), 1.97 (t, $J = 8.0$ Hz, 2H), 1.82–1.74 (m, 2H).

methyl 4-((6-(3,6-diacetyl-9H-carbazol-9-yl)hexanamido)methyl)benzoate (5e)

White solid. Mp:199–200 °C. ^1H NMR (400 MHz, Chloroform-*d*) δ 8.79 (d, $J = 1.8$ Hz, 2H), 8.17 (dd, $J = 8.7$, 1.7 Hz, 2H), 7.98 (d, $J = 8.0$ Hz, 2H), 7.44 (d, $J = 8.7$ Hz, 2H), 7.30 (d, $J = 8.0$ Hz, 2H), 5.71 (s, 1H), 4.46 (d, $J = 6.0$ Hz, 2H), 4.37 (t, $J = 7.1$ Hz, 2H), 3.91 (s, 3H), 2.74 (s, 6H), 2.19 (t, $J = 7.3$ Hz, 2H), 1.94 (p, $J = 7.4$ Hz, 2H), 1.73 (p, $J = 7.5$ Hz, 2H), 1.42 (p, $J = 8.0$ Hz, 2H).

methyl 4-((7-(3,6-diacetyl-9H-carbazol-9-yl)heptanamido)methyl)benzoate (5f)

White solid. Mp:194–195 °C. ^1H NMR (400 MHz, Chloroform-*d*) δ 8.79 (d, $J = 1.7$ Hz, 2H), 8.18 (dd, $J = 8.7$, 1.7 Hz, 2H), 7.98 (d, $J = 8.2$ Hz, 2H), 7.45 (d, $J = 8.7$ Hz, 2H), 7.31 (d, $J = 8.0$ Hz, 2H), 5.72 (s, 1H), 4.47 (d, $J = 5.9$ Hz, 2H), 4.35 (t, $J = 7.1$ Hz, 2H), 3.90 (s, 3H), 2.75 (s, 6H), 2.18 (t, $J = 7.4$ Hz, 2H), 1.98–1.86 (m, 2H), 1.73 – 1.61 (m, 2H), 1.46–1.32 (m, 4H).

methyl 4-((8-(3,6-diacetyl-9H-carbazol-9-yl)octanamido)methyl)benzoate (5g)

White solid. Mp:180–181 °C. ^1H NMR (400 MHz, Chloroform-*d*) δ 8.80 (d, $J = 1.7$ Hz, 2H), 8.18 (dd, $J = 8.7$, 1.7 Hz, 2H), 7.99 (d, $J = 8.1$ Hz, 2H), 7.46 (d, $J = 8.7$ Hz, 2H), 7.32 (d, $J = 8.0$ Hz, 2H), 5.73 (s, 1H), 4.48 (d, $J = 5.9$ Hz, 2H), 4.35 (t, $J = 7.2$ Hz, 2H), 3.91 (s, 3H), 2.75 (s, 6H), 2.19 (t, $J = 7.5$ Hz, 2H), 1.88 (d, $J = 7.6$ Hz, 2H), 1.69 – 1.60 (m, 2H), 1.40–1.25 (m, 6H).

6a–6g were synthesized in the same way as **3a**.

4-((2-(3,6-diacetyl-9H-carbazol-9-yl)acetamido)methyl)-N-hydroxybenzamide (6a)

White solid. Mp: 226–227 °C. ¹H NMR (400 MHz, DMSO-*d*₆) δ 8.51–8.46 (m, 2H), 7.89 (d, *J* = 7.9 Hz, 1H), 7.84 (d, *J* = 8.6 Hz, 2H), 7.71 (d, *J* = 7.9 Hz, 1H), 7.57 (d, *J* = 8.7 Hz, 2H), 7.39 (d, *J* = 8.0 Hz, 1H), 7.34 (d, *J* = 7.9 Hz, 1H), 5.18 (s, 2H), 4.36 (dd, *J* = 12.4, 5.8 Hz, 2H), 2.30 (s, 6H). ¹³C NMR (101 MHz, DMSO) δ 167.99, 167.62, 153.93, 144.79, 141.69, 129.80, 129.20, 127.71, 127.52, 124.00, 122.83, 118.54, 109.98, 46.22, 42.54, 12.44. HRMS (ESI) *m/z* Calcd [M + H]⁺ 458.1710, found: 458.1711.

4-((3-(3,6-diacetyl-9H-carbazol-9-yl)propanamido)methyl)-N-hydroxybenzamide (6b)

White solid. Mp: 202–204 °C. ¹H NMR (400 MHz, DMSO-*d*₆) δ 8.48 (d, *J* = 2.1 Hz, 2H), 7.85 (dd, *J* = 8.7, 2.0 Hz, 2H), 7.66 (d, *J* = 8.0 Hz, 1H), 7.62 (d, *J* = 8.7 Hz, 2H), 7.54 (d, *J* = 7.9 Hz, 1H), 7.00 (d, *J* = 7.9 Hz, 1H), 6.95 (d, *J* = 8.0 Hz, 1H), 4.68 (t, *J* = 6.4 Hz, 2H), 4.20 (d, *J* = 6.3 Hz, 2H), 2.70 (q, *J* = 7.1, 6.6 Hz, 2H), 2.31 (s, 6H). ¹³C NMR (101 MHz, DMSO) δ 170.57, 153.95, 153.92, 144.55, 142.76, 140.77, 129.61, 128.98, 127.40, 127.24, 123.96, 122.71, 118.56, 110.16, 110.09, 42.27, 35.38, 12.40. HRMS (ESI) *m/z* Calcd [M + H]⁺ 472.1867, found: 472.1866.

4-((4-(3,6-diacetyl-9H-carbazol-9-yl)butanamido)methyl)-N-hydroxybenzamide (6c)

White solid. Mp: 170–172 °C. ¹H NMR (400 MHz, DMSO-*d*₆) δ 8.48 (d, *J* = 1.8 Hz, 2H), 7.85 (dd, *J* = 8.8, 1.8 Hz, 2H), 7.69 (d, *J* = 7.9 Hz, 2H), 7.60 (d, *J* = 8.7 Hz, 2H), 7.29 (d, *J* = 7.9 Hz, 2H), 4.43 (t, *J* = 7.1 Hz, 2H), 4.28 (d, *J* = 5.9 Hz, 2H), 2.30 (s, 6H), 2.27–2.19 (m, 2H), 2.09–1.99 (m, 2H). ¹³C NMR (101 MHz, DMSO) δ 172.01, 153.92, 143.34, 140.98, 131.73, 129.82, 128.87, 127.72, 127.56, 127.38, 124.02, 122.59, 118.63, 109.81, 42.33, 32.53, 25.00, 12.40. HRMS (ESI) *m/z* Calcd [M + H]⁺ 486.2023, found: 486.2028.

4-((5-(3,6-diacetyl-9H-carbazol-9-yl)pentanamido)methyl)-N-hydroxybenzamide (6d)

White solid. Mp: 151–153 °C. ¹H NMR (400 MHz, DMSO-*d*₆) δ 10.97 (s, 2H), 8.47 (d, *J* = 1.8 Hz, 2H), 7.85 (dd, *J* = 8.5, 1.8 Hz, 4H), 7.61 (d, *J* = 8.8 Hz, 2H), 7.30 (d, *J* = 8.0 Hz, 2H), 4.43 (t, *J* = 6.9 Hz, 2H), 4.28 (d, *J* = 5.9 Hz, 2H), 2.30 (s, 6H), 2.18 (t, *J* = 7.3 Hz, 2H), 2.08 (s, 2H), 1.78 (s, 2H), 1.60–1.54 (m, 2H). ¹³C NMR (101 MHz, DMSO) δ 172.49, 167.68, 153.94, 145.19, 140.98, 129.79, 128.80, 127.55, 123.99, 122.54, 118.60,

109.85, 42.70, 42.24, 35.42, 28.72, 23.35, 12.38. HRMS (ESI) *m/z* Calcd [M + H]⁺ 500.2180, found: 500.2183.

4-((6-(3,6-diacetyl-9H-carbazol-9-yl)hexanamido)methyl)-N-hydroxybenzamide (6e)

White solid. Mp: 184–186 °C. ¹H NMR (400 MHz, DMSO-*d*₆) δ 8.47 (s, 2H), 7.91–7.81 (m, 3H), 7.70 (d, *J* = 7.9 Hz, 1H), 7.59 (d, *J* = 8.7 Hz, 2H), 7.31 (d, *J* = 7.9 Hz, 1H), 7.27 (d, *J* = 7.9 Hz, 1H), 4.46–4.36 (m, 2H), 4.26 (dd, *J* = 12.2, 5.9 Hz, 2H), 2.30 (s, 6H), 2.10 (t, *J* = 7.6 Hz, 2H), 1.79 (d, *J* = 8.9 Hz, 2H), 1.60–1.49 (m, 2H), 1.34–1.24 (m, 2H). ¹³C NMR (101 MHz, DMSO) δ 172.60, 167.64, 153.91, 145.40, 140.98, 129.82, 128.78, 127.61, 127.45, 123.98, 122.54, 118.63, 109.84, 42.88, 42.24, 35.60, 28.84, 26.59, 25.47, 12.38. HRMS (ESI) *m/z* Calcd [M + H]⁺ 514.2336, found: 514.2332.

4-((7-(3,6-diacetyl-9H-carbazol-9-yl)heptanamido)methyl)-N-hydroxybenzamide (6f)

White solid. Mp: 172–174 °C. ¹H NMR (400 MHz, DMSO-*d*₆) δ 8.47 (s, 2H), 7.86 (d, *J* = 8.4 Hz, 2H), 7.69 (d, *J* = 8.0 Hz, 2H), 7.60 (d, *J* = 8.7 Hz, 2H), 7.28 (d, *J* = 7.9 Hz, 2H), 4.39 (t, *J* = 7.0 Hz, 2H), 4.26 (d, *J* = 5.8 Hz, 2H), 2.30 (s, 6H), 2.10 (t, *J* = 7.2 Hz, 2H), 1.77 (t, *J* = 7.2 Hz, 2H), 1.47 (t, *J* = 7.0 Hz, 2H), 1.36–1.23 (m, 4H). ¹³C NMR (101 MHz, DMSO) δ 172.65, 153.92, 143.52, 141.00, 131.68, 129.81, 128.78, 127.44, 127.37, 124.00, 122.54, 118.63, 109.83, 42.91, 42.19, 35.71, 28.96, 28.93, 26.68, 25.60, 12.38. HRMS (ESI) *m/z* Calcd [M + H]⁺ 526.2347, found: 526.2377.

4-((8-(3,6-diacetyl-9H-carbazol-9-yl)octanamido)methyl)-N-hydroxybenzamide (6g)

White solid. Mp: 213–214 °C. ¹H NMR (400 MHz, DMSO-*d*₆) δ 8.47 (s, 2H), 7.93–7.81 (m, 4H), 7.60 (d, *J* = 8.7 Hz, 2H), 7.33 (d, *J* = 7.9 Hz, 2H), 4.40 (t, *J* = 7.0 Hz, 2H), 4.30 (d, *J* = 5.9 Hz, 2H), 2.30 (s, 6H), 2.11 (t, *J* = 7.4 Hz, 2H), 1.82–1.71 (m, 2H), 1.48 (t, *J* = 7.5 Hz, 2H), 1.34–1.24 (m, 4H), 1.22–1.14 (m, 2H). ¹³C NMR (101 MHz, DMSO) δ 172.78, 167.65, 153.93, 145.46, 140.99, 129.80, 129.69, 128.76, 127.62, 123.98, 122.52, 118.62, 109.82, 42.92, 42.24, 35.71, 29.03, 28.94, 26.83, 25.67, 12.37. HRMS (ESI) *m/z* Calcd [M + H]⁺ 542.2649, found: 542.2656.

7a–7g were synthesized in the same way as **5a**.

ethyl (E)-3-(4-((2-(3,6-diacetyl-9H-carbazol-9-yl)acetamido)methyl)phenyl)acrylate (7a)

White solid. Mp: 238–240 °C. ¹H NMR (400 MHz, Chloroform-*d*) δ 8.66 (s, 2H), 8.10 (dd, *J* = 8.6, 1.6 Hz,

1H), 7.50 (d, $J = 16.0$ Hz, 1H), 7.38 (d, $J = 8.6$ Hz, 2H), 7.30 (d, $J = 7.9$ Hz, 2H), 7.02 (d, $J = 7.9$ Hz, 2H), 6.28 (d, $J = 16.1$ Hz, 1H), 6.02 (s, 1H), 4.99 (s, 2H), 4.34 (d, $J = 6.0$ Hz, 2H), 4.17 (d, $J = 7.2$ Hz, 2H), 2.63 (s, 6H), 1.25 (t, $J = 7.1$ Hz, 3H).

ethyl (E)-3-(4-((3-(3,6-diacetyl-9H-carbazol-9-yl)propanamido)methyl)phenyl)acrylate (7b)

White solid. Mp:232–233 °C. ^1H NMR (400 MHz, Chloroform-*d*) δ 8.77 (d, $J = 1.7$ Hz, 2H), 8.14 (dd, $J = 8.7$, 1.7 Hz, 2H), 7.62–7.48 (m, 3H), 7.28 (d, $J = 8.3$ Hz, 2H), 6.92 (d, $J = 7.9$ Hz, 2H), 6.34 (d, $J = 16.0$ Hz, 1H), 5.71 (s, 1H), 4.79 (t, $J = 6.4$ Hz, 2H), 4.27 (dd, $J = 9.2$, 6.4 Hz, 4H), 2.79 (t, $J = 6.5$ Hz, 2H), 2.72 (s, 6H), 1.34 (t, $J = 7.1$ Hz, 3H).

Ethyl (E)-3-(4-((4-(3,6-diacetyl-9H-carbazol-9-yl)butanamido)methyl)phenyl)acrylate (7c)

White solid. Mp:221–222 °C. ^1H NMR (400 MHz, Chloroform-*d*) δ 8.76 (d, $J = 1.7$ Hz, 2H), 8.12 (dd, $J = 8.6$, 1.7 Hz, 2H), 7.64 (d, $J = 16.0$ Hz, 1H), 7.48 (dd, $J = 8.3$, 2.5 Hz, 4H), 7.29 (d, 2H), 6.41 (d, $J = 16.1$ Hz, 1H), 5.74 (t, $J = 5.9$ Hz, 1H), 4.50 (t, $J = 6.7$ Hz, 2H), 4.45 (d, $J = 5.8$ Hz, 2H), 4.25 (q, $J = 7.2$ Hz, 2H), 2.72 (s, 6H), 2.29 (q, $J = 6.7$ Hz, 2H), 2.22 (t, $J = 6.4$ Hz, 2H), 1.33 (t, $J = 7.1$ Hz, 3H).

ethyl (E)-3-(4-((5-(3,6-diacetyl-9H-carbazol-9-yl)pentanamido)methyl)phenyl)acrylate (7d)

White solid. Mp:201–202 °C. ^1H NMR (400 MHz, Chloroform-*d*) δ 8.79 (d, $J = 1.8$ Hz, 2H), 8.17 (dd, $J = 8.7$, 1.7 Hz, 2H), 7.63 (d, $J = 16.0$ Hz, 1H), 7.45 (dd, $J = 12.5$, 8.4 Hz, 4H), 7.23 (d, $J = 7.9$ Hz, 2H), 6.39 (d, $J = 16.0$ Hz, 1H), 4.40 (t, $J = 6.7$ Hz, 4H), 4.26 (q, $J = 7.2$ Hz, 2H), 2.74 (s, 6H), 2.22 (t, $J = 7.2$ Hz, 2H), 1.95 (d, $J = 8.2$ Hz, 2H), 1.77 (t, $J = 7.9$ Hz, 2H), 1.34 (t, $J = 7.1$ Hz, 3H).

ethyl (E)-3-(4-((6-(3,6-diacetyl-9H-carbazol-9-yl)hexanamido)methyl)phenyl)acrylate (7e)

White solid. Mp:189–190 °C. ^1H NMR (400 MHz, Chloroform-*d*) δ 8.79 (d, $J = 1.8$ Hz, 2H), 8.17 (dd, $J = 8.7$, 1.7 Hz, 2H), 7.65 (d, $J = 16.0$ Hz, 1H), 7.46 (t, $J = 8.8$ Hz, 4H), 7.24 (d, 2H), 6.41 (d, $J = 16.0$ Hz, 1H), 5.65 (s, 1H), 4.42 (d, $J = 5.9$ Hz, 2H), 4.37 (t, $J = 7.1$ Hz, 2H), 4.26 (q, $J = 7.1$ Hz, 2H), 2.74 (s, 6H), 2.18 (t, $J = 7.4$ Hz, 2H), 1.93 (t, $J = 7.7$ Hz, 2H), 1.72 (q, $J = 7.6$ Hz, 2H), 1.43 (q, $J = 8.3$ Hz, 2H), 1.34 (t, $J = 7.1$ Hz, 3H).

ethyl (E)-3-(4-((7-(3,6-diacetyl-9H-carbazol-9-yl)heptanamido)methyl)phenyl)acrylate (7f)

White solid. Mp:159–160 °C. ^1H NMR (400 MHz, Chloroform-*d*) δ 8.80 (d, $J = 1.7$ Hz, 2H), 8.18 (dd, $J = 8.7$, 1.7 Hz, 2H), 7.63 (d, $J = 16.0$ Hz, 1H), 7.46 (dd, $J = 8.4$, 3.5 Hz, 4H), 7.27 (d, 2H), 6.39 (d, $J = 16.0$ Hz, 1H), 5.67 (s, 1H), 4.42 (d, $J = 5.8$ Hz, 2H), 4.35 (t, $J = 7.2$ Hz, 2H), 4.26 (q, $J = 7.2$ Hz, 2H), 2.75 (s, 6H), 2.17 (t, $J = 7.4$ Hz, 2H), 1.91 (t, $J = 7.1$ Hz, 2H), 1.64 (t, $J = 7.3$ Hz, 2H), 1.43–1.30 (m, 7H).

ethyl (E)-3-(4-((8-(3,6-diacetyl-9H-carbazol-9-yl)octanamido)methyl)phenyl)acrylate (7g)

White solid. Mp:150–151 °C. ^1H NMR (400 MHz, Chloroform-*d*) δ 8.80 (d, $J = 1.7$ Hz, 2H), 8.18 (dd, $J = 8.6$, 1.7 Hz, 2H), 7.65 (d, $J = 16.0$ Hz, 1H), 7.46 (dd, $J = 8.4$, 3.7 Hz, 4H), 7.28 (d, 2H), 6.41 (d, $J = 16.0$ Hz, 1H), 4.44 (d, $J = 5.8$ Hz, 2H), 4.35 (t, $J = 7.2$ Hz, 2H), 4.26 (q, $J = 7.1$ Hz, 2H), 2.75 (s, 6H), 2.18 (t, $J = 7.5$ Hz, 2H), 1.88 (d, $J = 8.1$ Hz, 2H), 1.62 (dd, $J = 15.0$, 7.7 Hz, 4H), 1.38–1.30 (m, 7H).

8a–8g were synthesized in the same way as **6a**.

(E)-3-(4-((2-(3,6-diacetyl-9H-carbazol-9-yl)acetamido)methyl)phenyl)-N-hydroxyacrylamide (8a)

White solid. Mp: 222–224 °C. ^1H NMR (400 MHz, DMSO-*d*₆) δ 8.48 (s, 2H), 7.84 (dd, $J = 8.7$, 1.8 Hz, 2H), 7.53 (dd, $J = 15.6$, 8.3 Hz, 4H), 7.43 (d, $J = 15.8$ Hz, 1H), 7.31 (d, $J = 7.8$ Hz, 2H), 6.47 (d, $J = 15.9$ Hz, 1H), 5.15 (s, 2H), 4.32 (d, $J = 5.8$ Hz, 2H), 2.30 (s, 6H). ^{13}C NMR (101 MHz, DMSO) δ 167.86, 163.28, 153.94, 141.70, 141.07, 138.44, 134.02, 129.18, 128.27, 127.92, 124.00, 122.82, 119.35, 118.52, 109.97, 46.22, 42.55, 12.44. HRMS (ESI) m/z Calcd $[\text{M} + \text{H}]^+$ 482.1940, found: 482.1945.

(E)-3-(4-((3-(3,6-diacetyl-9H-carbazol-9-yl)propanamido)methyl)phenyl)-N-hydroxyacrylamide (8b)

White solid. Mp: 112–113 °C. ^1H NMR (400 MHz, DMSO-*d*₆) δ 8.49 (s, 2H), 8.40 (t, $J = 6.0$ Hz, 1H), 7.90 – 7.81 (m, 2H), 7.61 (d, $J = 8.7$ Hz, 2H), 7.48 (d, $J = 16.0$ Hz, 1H), 7.40 (d, $J = 7.8$ Hz, 2H), 6.92 (d, $J = 8.0$ Hz, 2H), 6.42 (d, $J = 16.0$ Hz, 1H), 4.69 (t, $J = 6.3$ Hz, 2H), 4.17 (d, $J = 5.9$ Hz, 2H), 2.69 (t, $J = 6.8$ Hz, 2H), 2.31 (s, 6H). ^{13}C NMR (101 MHz, DMSO) δ 197.57, 168.01, 153.91, 144.03, 143.76, 140.76, 129.96, 129.92, 128.97, 128.41, 127.86, 126.89, 123.94, 122.98, 122.88, 122.73, 119.14, 118.57, 110.59, 72.09, 42.27, 27.21, 12.39. HRMS (ESI) m/z Calcd $[\text{M} + \text{H}]^+$ 498.2023, found: 498.2025.

(E)-4-(3,6-diacetyl-9H-carbazol-9-yl)-N-(4-(3-(hydroxyamino)-3-oxoprop-1-en-1-yl)benzyl)butanamide (8c)

White solid. Mp: 154–156 °C. ¹H NMR (400 MHz, DMSO-*d*₆) δ 8.48 (s, 2H), 8.42 (d, *J* = 5.9 Hz, 1H), 7.84 (d, *J* = 8.6 Hz, 2H), 7.64 – 7.56 (m, 3H), 7.49 (d, *J* = 7.6 Hz, 1H), 7.41 (d, *J* = 15.7 Hz, 1H), 7.26 (d, *J* = 7.8 Hz, 2H), 6.52–6.42 (m, 1H), 4.43 (t, *J* = 7.0 Hz, 2H), 4.26 (d, *J* = 5.7 Hz, 2H), 2.30 (s, 6H), 2.20 (d, *J* = 7.2 Hz, 2H), 2.03 (t, *J* = 7.2 Hz, 2H). ¹³C NMR (101 MHz, DMSO) δ 171.96, 163.21, 153.84, 140.98, 138.37, 133.90, 128.86, 128.44, 128.28, 127.91, 124.01, 122.58, 119.29, 118.62, 109.80, 42.48, 32.50, 24.98, 12.39. HRMS (ESI) *m/z* Calcd [M + H]⁺ 512.2180, found: 512.2187.

(E)-5-(3,6-diacetyl-9H-carbazol-9-yl)-N-(4-(3-(hydroxyamino)-3-oxoprop-1-en-1-yl)benzyl)pentanamide (8d)

White solid. Mp: 152–153 °C. ¹H NMR (400 MHz, DMSO-*d*₆) δ 8.52–8.44 (m, 2H), 8.32 (s, 1H), 7.85 (dd, *J* = 8.7, 1.8 Hz, 2H), 7.61 (d, *J* = 8.8 Hz, 2H), 7.49–7.40 (m, 2H), 7.20 (d, *J* = 7.8 Hz, 2H), 6.41 (d, *J* = 15.8 Hz, 1H), 4.42 (d, *J* = 7.6 Hz, 2H), 4.22 (d, *J* = 5.8 Hz, 2H), 2.30 (s, 6H), 2.17 (t, *J* = 7.4 Hz, 2H), 1.77 (dd, *J* = 12.4, 6.6 Hz, 2H), 1.63–1.49 (m, 2H). ¹³C NMR (101 MHz, DMSO) δ 172.38, 163.36, 153.97, 141.63, 140.99, 138.63, 133.81, 128.81, 128.08, 127.91, 124.00, 122.56, 119.05, 118.64, 109.85, 42.73, 42.22, 35.50, 28.76, 23.44, 12.40. HRMS (ESI) *m/z* Calcd [M + H]⁺ 524.2336, found: 524.2359.

(E)-6-(3,6-diacetyl-9H-carbazol-9-yl)-N-(4-(3-(hydroxyamino)-3-oxoprop-1-en-1-yl)benzyl)hexanamide (8e)

White solid. Mp: 121–123 °C. ¹H NMR (400 MHz, DMSO-*d*₆) δ 8.48 (s, 2H), 8.28 (t, *J* = 5.7 Hz, 1H), 7.90 – 7.79 (m, 2H), 7.59 (d, *J* = 8.7 Hz, 2H), 7.52–7.45 (m, 2H), 7.41 (d, 1H), 7.23 (d, *J* = 7.8 Hz, 2H), 6.43 (d, *J* = 15.8 Hz, 1H), 4.45–4.33 (m, 2H), 4.21 (d, *J* = 5.8 Hz, 2H), 2.30 (s, 6H), 2.09 (t, *J* = 7.4 Hz, 2H), 1.77 (d, *J* = 7.7 Hz, 2H), 1.64–1.44 (m, 2H), 1.29 (d, *J* = 10.3 Hz, 2H). ¹³C NMR (101 MHz, DMSO) δ 172.51, 163.25, 153.94, 141.68, 140.99, 138.47, 133.84, 128.76, 128.14, 127.90, 123.99, 122.54, 119.18, 118.62, 109.84, 42.90, 42.23, 35.61, 28.85, 26.59, 25.47, 12.38. HRMS (ESI) *m/z* Calcd [M + H]⁺ 538.2347, found: 538.2372.

(E)-7-(3,6-diacetyl-9H-carbazol-9-yl)-N-(4-(3-(hydroxyamino)-3-oxoprop-1-en-1-yl)benzyl)heptanamide (8f)

White solid. Mp: 113–115 °C. ¹H NMR (400 MHz, DMSO-*d*₆) δ 8.47 (d, *J* = 1.8 Hz, 2H), 8.29 (d, *J* = 6.1 Hz, 1H), 7.85 (dd, *J* = 8.7, 1.8 Hz, 2H), 7.60 (d, *J* = 8.7 Hz, 2H), 7.48 (d, *J* = 7.8 Hz, 2H), 7.42 (d, *J* = 15.8 Hz, 1H), 7.24 (d, *J* = 7.9 Hz, 2H), 6.42 (d, *J* = 15.8 Hz, 1H), 4.39 (t, *J* = 7.0 Hz, 2H), 4.23 (d, *J* = 5.9 Hz, 2H), 2.30 (s, 6H), 2.09 (t, *J* = 7.3 Hz, 2H), 1.77 (s, 2H), 1.52 – 1.40 (m, 2H), 1.35–1.21 (m, 4H). ¹³C NMR (101 MHz, DMSO) δ 172.61, 163.31, 153.94, 141.75, 141.00, 138.53, 133.82, 128.78, 128.14, 127.90, 123.99, 122.54, 119.15, 118.62, 109.82, 60.22, 42.91, 42.23, 35.72, 28.93, 26.65, 25.60, 12.38. HRMS (ESI) *m/z* Calcd [M + H]⁺ 552.2504, found: 552.2514.

(E)-8-(3,6-diacetyl-9H-carbazol-9-yl)-N-(4-(3-(hydroxyamino)-3-oxoprop-1-en-1-yl)benzyl)octanamide (8g)

White solid. Mp: 167–168 °C. ¹H NMR (400 MHz, DMSO-*d*₆) δ 8.47 (d, *J* = 1.7 Hz, 2H), 8.31 (d, *J* = 6.2 Hz, 1H), 7.85 (dd, *J* = 8.7, 1.8 Hz, 2H), 7.60 (d, *J* = 8.7 Hz, 2H), 7.47 (d, *J* = 7.9 Hz, 2H), 7.40 (d, *J* = 15.3 Hz, 1H), 7.23 (d, *J* = 7.9 Hz, 2H), 6.47 (d, *J* = 15.9 Hz, 1H), 4.40 (t, *J* = 7.0 Hz, 2H), 4.23 (d, *J* = 5.9 Hz, 2H), 2.30 (s, 6H), 2.09 (t, *J* = 7.4 Hz, 2H), 1.76 (s, 2H), 1.47 (q, *J* = 7.4 Hz, 2H), 1.27 (s, 4H), 1.19 (s, 2H). ¹³C NMR (101 MHz, DMSO) δ 172.65, 163.27, 153.89, 141.54, 140.99, 137.72, 134.03, 128.77, 128.12, 127.79, 123.97, 122.53, 119.69, 118.62, 109.83, 42.93, 42.29, 35.72, 29.03, 26.84, 25.68, 12.36. HRMS (ESI) *m/z* Calcd [M + H]⁺ 568.2805, found: 568.2800.

HeLa nuclear extract and HDAC enzymatic assay

The mixed solution containing enzyme solution (HeLa nuclear extract, HDAC1, HDAC6 or HDAC8), the tested compounds solution and the fluorogenic substrate solution [Boc-Lys (acetyl)-AMC or Boc-Lys (trifluoroacetyl)-AMC] were plated to enzyme-labeled plate. After incubation (30 min, 37 °C), the reaction was stopped by the trypsin and trichostatin A. Fluorescence was analyzed with EX/EM 360/460 nm by Microplate reader (Tecan).

In vitro antiproliferative activity

HCT-116, HepG2, HeLa, HEL, Molt-4, and U266 cells were treated with different concentrations of compounds after

seeded into 96-well plates, respectively. After co-incubation for 48 h, 20 μ l CCK8 was added to each well and incubated for 4 h at 37 °C. Microplate reader (Tecan) was used to detect the absorbance at 450 nm for each well.

Flow cytometric assay

Molt4 cells were treated with **3g** (0.5 μ M, 1.5 μ M) for 24 h. Then the cells were collected pellets for annexin V-FITC/PI staining. The stained cells were analyzed by a flow cytometer.

Western blot assay

Molt4 cancer cells were treated with **3g** (0.17 μ M, 0.5 μ M, 1.5 μ M) for 24 h, then the cells were collected pellets for protein extraction. The protein content was determined by the BCA protein determination assay. Equal amounts of the total protein were measured for Western blot, such as Ac-HH3, Ac-Tubulin and cleaved caspase 3.

Molecular docking

The crystal structures of HDAC1 (PDB code: 5ICN) were downloaded from Protein Data Bank. Molecular docking was conducted using the MOE software. The top-scored results were selected as the most favorable binding model.

Funding This work was supported by the Key Research and Development Program of Shandong Province (No. 2019JZZY011115 and 2021CXGC011101), Weihai Zhengsheng Biotechnology Foundation and Rongxiang Regenerative Medicine Foundation of Shandong University (No. 2019SDRX-05), National Natural Science Foundation of China (22101146), Natural Science Foundation of Shandong Province (ZR2020QB005), Weihai-Shandong Academy of Sciences Industry University research collaborative innovation fund (2020CXY08, 2020GC04).

Compliance with ethical standards

Conflict of interest The authors declare no competing interests.

References

- Khan O, La Thangue NB. HDAC inhibitors in cancer biology: emerging mechanisms and clinical applications. *Immunol Cell Biol.* 2012;90:85–94. <https://doi.org/10.1038/icb.2011.100>.
- Bajbouj K, Al-Ali A, Ramakrishnan RK, Saber-Ayad M, Hamid Q. Histone modification in NSCLC: molecular mechanisms and therapeutic targets. *Int J Mol Sci.* 2021;22:11701 <https://doi.org/10.3390/ijms222111701>.
- Kunadis E, Lakiotaki E, Korkolopoulou P, Piperi C. Targeting post-translational histone modifying enzymes in glioblastoma. *Pharmacol Ther.* 2021;220:107721 <https://doi.org/10.1016/j.pharmthera.2020.107721>.
- Abu-Zhayia ER, Machour FE, Ayoub N. HDAC-dependent decrease in histone crotonylation during DNA damage. *J Mol Cell Biol.* 2019;11:804–6. <https://doi.org/10.1093/jmcb/mjz019>.
- Liang T, Zhou Y, Elhassan RM, Hou X, Yang X, Fang H. HDAC–Bax multiple ligands enhance Bax-dependent apoptosis in Hela cells. *J Med Chem.* 2020;63:12083–99. <https://doi.org/10.1021/acs.jmedchem.0c01454>.
- Punpai S, Saenkham A, Jarintanan F, Jongrungruangchok S, Choowongkamon K, Suksamrarn S, et al. HDAC inhibitor cow-anin extracted from *G. fusca* induces apoptosis and autophagy via inhibition of the PI3K/Akt/mTOR pathways in Jurkat cells. *Biomed Pharmacother.* 2022;147:112577 <https://doi.org/10.1016/j.biopha.2021.112577>.
- Cui H, Hong Q, Wei R, Li H, Wan C, Chen X, et al. Design and synthesis of HDAC inhibitors to enhance the therapeutic effect of diffuse large B-cell lymphoma by improving metabolic stability and pharmacokinetic characteristics. *Eur J Med Chem.* 2022;229:114049 <https://doi.org/10.1016/j.ejmech.2021.114049>.
- Liu M, Gao S, Liang T, Qiu X, Yang X, Fang H, et al. Discovery of novel Src homology-2 domain-containing phosphatase 2 and histone deacetylase dual inhibitors with potent antitumor efficacy and enhanced antitumor immunity. *J Med Chem.* 2022;65:12200–18. <https://doi.org/10.1021/acs.jmedchem.2c00866>.
- Vaidya GN, Rana P, Venkatesh A, Chatterjee DR, Contractor D, Satpute DP, et al. Paradigm shift of “classical” HDAC inhibitors to “hybrid” HDAC inhibitors in therapeutic interventions. *Eur J Med Chem.* 2021;209:112844 <https://doi.org/10.1016/j.ejmech.2020.112844>.
- Hesham HM, Lasheen DS, Abouzid KAM. Chimeric HDAC inhibitors: comprehensive review on the HDAC-based strategies developed to combat cancer. *Med Res Rev.* 2018;38:2058–109. <https://doi.org/10.1002/med.21505>.
- Huang L, Feng Z-L, Wang Y-T, Lin L-G. Anticancer carbazole alkaloids and coumarins from *Clausena* plants: a review. *Chin J Nat Med.* 2017;15:881–8. [https://doi.org/10.1016/S1875-5364\(18\)30003-7](https://doi.org/10.1016/S1875-5364(18)30003-7).
- Gluszyńska A. Biological potential of carbazole derivatives. *Eur J Med Chem.* 2015;94:405–26. <https://doi.org/10.1016/j.ejmech.2015.02.059>.
- Humphries PS, Bersot R, Kincaid J, Mabery E, McCluskie K, Park T, et al. Carbazole-containing amides and ureas: discovery of cryptochrome modulators as antihyperglycemic agents. *Bioorg Med Chem Lett.* 2018;28:293–7. <https://doi.org/10.1016/j.bmcl.2017.12.051>.
- Chen C, Chu H, Wang A, Yin H, Gao Y, Liu S, et al. Discovery of 2,5-diphenyl-1,3,4-thiadiazole derivatives as HDAC inhibitors with DNA binding affinity. *Eur J Med Chem.* 2022;241:114634 <https://doi.org/10.1016/j.ejmech.2022.114634>.
- Chen C, Hou X, Wang G, Pan W, Yang X, Zhang Y, et al. Design, synthesis and biological evaluation of quinoline derivatives as HDAC class I inhibitors. *Eur J Med Chem.* 2017;133:11–23. <https://doi.org/10.1016/j.ejmech.2017.03.064>.
- Chen C, Li X, Zhao H, Liu M, Du J, Zhang J, et al. Discovery of DNA-targeting HDAC inhibitors with potent antitumor efficacy in vivo that trigger antitumor immunity. *J Med Chem.* 2022;65:3667–83. <https://doi.org/10.1021/acs.jmedchem.1c02225>.
- Velasco D, Castellanos S, López M, López-Calahorra F, Brillas E, Juliá L. Red organic light-emitting radical adducts of carbazole and tris(2,4,6-trichlorotriphenyl)methyl radical that exhibit high

thermal stability and electrochemical amphotericity. *J Org Chem.* 2007;72:7523–32. <https://doi.org/10.1021/jo0708846>.

Publisher's note Springer Nature remains neutral with regard to jurisdictional claims in published maps and institutional affiliations.

Springer Nature or its licensor (e.g. a society or other partner) holds exclusive rights to this article under a publishing agreement with the author(s) or other rightsholder(s); author self-archiving of the accepted manuscript version of this article is solely governed by the terms of such publishing agreement and applicable law.